Supplement of Atmos. Chem. Phys., 21, 12141–12153, 2021
https://doi.org/10.5194/acp-21-12141-2021-supplement

Supplement of

Gas–particle partitioning of polyol tracers at a suburban site in Nanjing, east China: increased partitioning to the particle phase

Chao Qin et al.

Correspondence to: Mingjie Xie (mingjie.xie@colorado.edu, mingjie.xie@nuist.edu.cn)

Text S1. Water uptake by water-soluble organic carbon (WSOC)

According to Isaacman-VanWertz et al. (2016), the water uptake by WSOC (W_{O}, μg m^{-3}) could be estimated as

$$W_{\mathrm{O}} = \frac{V_{\mathrm{WSOC}} \times \kappa}{(\frac{100}{\mathrm{RH\%}} - 1)} \qquad (1)$$

where V_{WSOC} represents WSOC volume, and is calculated as the organic mass (WSOC ×1.6) divided by its density (1.4 g cm^{-3}). The hygroscopicity parameter (κ) of secondary organic aerosol (SOA) was observed to increase as a function of its oxygen to carbon ratio (O:C; Massoli et al., 2010). Isaacman-VanWertz et al. (2016) estimated κ of hygroscopic organic matter by assuming a linear regression slope of 0.29 between κ and O:C. In previous field and laboratory studies, κ values of hygroscopic organic matter typically varied from 0.05 to 0.25 with a O:C range of 0.3–1.0 (Chang et al., 2010; Massoli et al., 2010; Taylor et al., 2017), and the corresponding average W_{O} based on Eq. S1 in this work ranged from 0.47 ± 1.14 to 2.34 ± 4.03 μg m^{-3}, far below the amount caused by inorganic ions (21.3 ± 24.2 μg m^{-3}, Table S1). Taylor et al. (2017) predicted a hygroscopic growth factor range of 1.00–1.20 with RH varying from 60 to ~100%, which lead to an average W_{O} of 0.42 ± 0.70 μg m^{-3} for this study. Thus, the water content contributed by WSOC was not accounted for in this work.

Text S2. Sample extraction and instrumental analysis

One eighth (25 cm^2) of each filter sample was spiked with 40 μL of internal standards solution (10 ng uL^{-1} of naphthalene-d8, acenaphthene-d10, phenanthrene-d10, chrysene-d10, and perylene-d12), followed by sonication in a mixture of methanol and methylene chloride (1:1, v/v) twice for 15 min each. All extracts were filtered through a prebaked glass fiber filter to a 100 mL pear shaped flask and rotary evaporated to ~0.5 mL. After that, the extract was transferred to a 2 mL glass vial and combined with 3 rinses of the flask using methanol and methylene chloride at a mixing ratio of 1:2. A gentle flow of N_2 was deployed to blow the concentrated extracts to dryness, and then 50 μL of N, O-bis(trimethylsilyl)trifluoroacetamide (BSTFA) containing 1% trimethylchlorosilane (TMCS) and 10 μL of pyridine were added to react with the dried extracts at 70 °C for 3 h. Prior to the analysis using gas chromatography (GC, Agilent 7890) – mass spectrometry (MS, Agilent 5977B), the cooled BSTFA:TMCS/pyridine solution was diluted to a final volume of 400 μL using pure *n*-hexane. Polyurethane foam (PUF) samples were pre-spiked using the same internal standard solution as that for filter samples, and were Soxhlet extracted using a mixture of methylene chloride (225 mL) and methanol (25 mL) for 24 h. The following pretreatment procedures were visualized in Figure S1, mostly the same as those for filter samples except that 50 μL of pure water was added to the derivatized and diluted extracts prior to GC-MS analysis. This additional step was supposed to separate PUF residues from polyol derivatives in the supernatant and avoid changing GC inlet liners too frequently.

An aliquot of 2 μL of each sample was analyzed using GC-MS under electron ionization mode (EI, 70 eV), and target polyols were separated with a HP-5ms capillary column (30 m × 0.25 mm × 0.25 μm). The GC oven temperature was initially held at 50 °C for 2 min, and then programmed to 120 °C at 3 °C min^{-1} (hold for 0 min) and 300 at 6 °C min^{-1} (final temperature, hold for 10 min). A six-point calibration curve (0.05 – 5 ng μl^{-1}) was generated using an internal standard method. The final concentrations of polyol tracers in each sample were derived from their total amount in sample extract and the sample volume. Due to the limited availability of authentic standards, secondary products of isoprene including C5-alkene triols (cis-2-methyl-1,3,4-trihydroxy-1-butene, 3-methyl-2,3,4-trihydroxy-1-butene, and trans-2-methyl-1,3,4-trihydroxy-1-butene; abbreviated as C5-alkene 1, 2, and 3) and 2-methyltetrols (2-methylthreitol and 2-methylerythritol) were quantified as meso-erythritol; sugars and sugar alcohols were quantified using authentic standards; other acid tracers (e.g., diacids, polyacids) were all quantified as ketopinic acid (Kleindienst et al., 2007), but were not reported here. Meso-erythritol and isoprene SOA tracers were expected to have different total ion intensity for the same amount, and the total ion signals of isoprene tracers in ambient air sample often co-eluted with other compounds, so the fragmentation difference between quantification ions of meso-erythritol (m/z 217) and isoprene SOA tracers (m/z 219) was not adjusted in this work. It should be noted that meso-erythritol was used as the surrogate for isoprene tracers without considering the fragmentation effect in a number of previous studies (Claeys et al., 2004; Hu et al., 2008; Ding et al., 2008, 2012; Lin et al., 2013; Xie et al., 2014b).

Text S3. Vapor pressure estimation

In eq. 3 of the main text, $p^{\mathrm{o}}{}_{\mathrm{L}}$ values of individual polyols for each sampling interval were adjusted by

$$p_{\mathrm{L}}^{\mathrm{o}} = p_{\mathrm{L}}^{\mathrm{o},*} \exp\left[\frac{\Delta H_{\mathrm{vap}}^{*}}{\mathrm{R}}\left(\frac{1}{298.15} - \frac{1}{\mathrm{T}}\right)\right] \qquad (2)$$

where $p^{\mathrm{o},*}{}_{\mathrm{L}}$ is the liquid-state vapor pressure and $\Delta H^{*}{}_{\mathrm{vap}}$ (kJ mol^{-1}) is the enthalpy of vaporization of the liquid at 298.15 K (Table S4). Due to the variability in $p^{\mathrm{o},*}{}_{\mathrm{L}}$ estimation, $p^{\mathrm{o},*}{}_{\mathrm{L}}$ values of polyol tracers in this study were estimated using several tools, including the Estimation Programs Interface (EPI) Suite developed by the US Environmental Protection Agency and Syracuse Research Corporation (US EPA, 2012), EVAPORATION (Compernolle et al., 2011), SPARC (Hilal et al., 2003), and SIMPOL (Pankow and Asher, 2008). $\Delta H^{*}{}_{\mathrm{vap}}$ values were estimated empirically from the correlation between $\Delta H^{*}{}_{\mathrm{vap}}$ and ln $p^{\mathrm{o},*}{}_{\mathrm{L}}$ (Goss and Schwarzenbach, 1999)

$$\Delta H_{\mathrm{vap}}^{*} = -3.82 Inp_{\mathrm{L}}^{\mathrm{o},*} + 70.0 \qquad (3)$$

Text S4. Prediction of Henry's law coefficient in pure water

The Henry's law coefficients of polyol tracers in pure water at 25 °C ($K^{*}{}_{\mathrm{H,w}}$, mol

m^{-3} atm^{-1}) were estimated using EPI and SPARC (Hilal et al., 2008), respectively (Table S4). Table S4 also provides $K^{*}_{H,w}$ values of isoprene SOA, levoglucosan and selected sugar polyols from literatures. Due to the variation in ambient temperature across air samples, predicted $K_{H,w}$ ($K^{t}_{H,w}$) values of polyol tracers were adjusted for each sample using van 't Hoff equation

$$K^{t}_{H,w} = K^{*}_{H,w} \exp\left[\frac{\Delta H^{*}_{sol}}{R}\left(\frac{1}{298.15} - \frac{1}{T}\right)\right] \quad (4)$$

where ΔH^{*}_{sol} (kJ mol^{-1}) refers to the enthalpy of dissolution at 298.15 K. The ΔH^{*}_{sol} values of meso-erythritol, xylitol, arabitol, and mannitol were obtained from Compernolle and Müller (2014), and were used as surrogates for other polyol compounds based on the number of hydroxyl groups. The ΔH^{*}_{sol} of C5-alkene triols were substituted by that of glycerol (92.6 kJ mol^{-1}; Compernolle and Müller, 2014).

Text S5. Uncertainty estimation methods

In this work, the measurement results of some polyol tracers in filter and PUF samples are subject to substantial uncertainties due to their low and variable recoveries (Table S2) and excessive breakthrough (Figure S2). A general equation was derived to estimate measurement uncertainties of individual polyols in filter and PUF samples

$$\Delta C = \sqrt{(\text{error fraction} \times \text{concentration})^2 + (0.5 \times \text{detection limit})^2} \quad (5)$$

where ΔC is the uncertainty of target species in filter (ΔQ_f and ΔQ_b, ng m^{-3}) or PUF (ΔPUF, ng m^{-3}) samples. The error fraction (%) of filter sample analysis was defined as half of the difference between maximum and minimum recoveries scaled by the average (Table S2), which was divided by (1 - average breakthrough) for PUF analysis (Figure S2). The average breakthrough of meso-erythritol (23.8%), mannose (38.1%), xylitol (36.4%), and arabitol (36.4%) were set as those of C5-alkene triols, glucose, and mannitol, respectively. According to the gas-particle separation method in this work, ΔQ_f was used to represent the uncertainty of particle-phase concentration (ΔF, ng m^{-3}), and the uncertainty of gas-phase concentration (ΔA, ng m^{-3}) was propagated by

$$\Delta A = \sqrt{{\Delta Q_b}^2 + \Delta PUF^2} \qquad (6)$$

Then the uncertainty of total concentration (ΔS, ng m^{-3}) was calculated as (Xie et al., 2013, 2014a)

$$\Delta S = \sqrt{\Delta F^2 + \Delta A^2} \qquad (7)$$

The uncertainties of particle-phase fractions (ΔF%) and partitioning coefficients ($K^{m}_{p,OM}$ and $K^{m}_{p,WIOM}$, m^3 ug^{-1}; $K^{m}_{H,e}$, mol m^{-3} atm^{-1}) were estimated by propagating ΔF, ΔS, and ΔA using a simplified root sum of squares (RSS) method (Dutton et al., 2009)

$$\Delta F\% = \sqrt{(\frac{\partial F\%}{\partial F}\Delta F)^2 + (\frac{\partial F\%}{\partial S}\Delta S)^2} \times 100\% \qquad (8)$$

$$\Delta K = \sqrt{(\frac{\partial K}{\partial F'}\Delta F')^2 + (\frac{\partial K}{\partial A}\Delta A)^2} \qquad (9)$$

where ΔK is the uncertainty of $K^{m}_{p,OM}$, $K^{m}_{p,WIOM}$, or $K^{m}_{H,e}$; F' could be F, concentrations of polyols in WIOM (F_{WIOM}) or aqueous (F_w) phases, depending on the partitioning scheme (*Cases 1–3*) and partitioning coefficient for calculation. ΔF was split into ΔFw and ΔF_{WIOM} (or ΔF_{OM}) based on their ratios in eq. 4 of the main text. In Table S5, the estimated uncertainties are summarized and expressed in average ratios. As $K^{m}_{p,OM}$ and $K^{m}_{H,e}$ are all directly related to the ratio of particle- (F, ng m^{-3}) and gas-phase (A, ng m^{-3}) concentrations (eqs. 2, 4, 5, and 6 in the main text), their average $\Delta K/K$ values are the same (Table S5).

Table S1. Statistics of ambient temperature (^{o}C), relative humidity (%), and $PM_{2.5}$ major species ($\mu g\ m^{-3}$) from Yang et al. (2021).

	Median	Mean ± stdev[a]	Range
Ambient temperature	18.2	17.9 ± 9.43	-4.18–36.1
Relative humidity	70.5	68.4 ± 17.6	24.5 – 99.5
$PM_{2.5}$	67.2	71.7 ± 34.5	18.9–165
NH_4^+	3.98	4.94 ± 3.31	1.08–21.7
NO_3^-	8.84	11.5 ± 10.4	0.12–53.2
SO_4^{2-}	7.54	8.70 ± 4.20	2.78–20.6
Ca^{2+}	1.35	1.85 ± 1.40	0.011–7.02
Mg^{2+}	0.10	0.13 ± 0.095	0.0088–0.43
K^+	0.77	1.00 ± 0.75	0.077–3.66
OC	6.82	7.61 ± 3.33	2.24–16.8
EC	2.83	2.93 ± 1.15	0.97–6.64
WSOC	3.93	4.35 ± 2.13	1.14–10.5
Aerosol liquid water[b]	12.2	21.3 ± 24.2	0.97–107

[a] Standard deviation; [b] predicted using ISORROPIA II model.

Table S2. Method detection limits (MDL, pg) and recoveries (%) of reference standards.

Polyol species	MDL	Filter (*N* = 6)		PUF (*N* = 6)	
		Average	Range	Average	Range
meso-erythritol	40.2	106 ± 1.90	102 – 108	50.7 ± 4.95	45.0 – 57.0
levoglucosan	43.8	99.3 ± 3.29	91.8 – 102	54.3 ± 5.92	46.5 – 63.9
fructose	54.9	79.3 ± 14.4	61.7 – 98.4	44.0 ± 13.2	30.4 – 57.9
mannose	46.4	79.9 ± 3.03	75.8 – 83.0	69.6 ± 10.5	57.2 – 84.5
glucose	88.3	100 ± 7.11	89.2 – 108	71.7 ± 22.3	53.8 – 109
xylitol	34.8	68.4 ± 5.68	61.6 – 75.8	44.9 ± 3.27	37.1 – 61.9
arabitol	42.6	75.8 ± 6.40	68.8 – 83.5	55.5 ± 8.21	45.1 – 67.7
mannitol	38.3	62.7 ± 9.02	48.5 – 74.9	55.3 ± 4.10	42.4 – 76.3

Table S3. Concentration statistics (ng m^{-3}) of target polyol tracers determined from filter and PUF samples.

Polyol species	Q_f				Q_b				PUF			
	No. of obs.	Median	Average ± Stdev	Range	No. of obs.	Median	Average ± Stdev	Range	No. of obs.	Median	Average ± Stdev	Range
Isoprene SOA tracers												
C5-alkene triol1	89	0.28	3.59 ± 10.0	0.013 – 69.4	56	0.056	0.14 ± 0.28	0.0046 – 1.86	31	0.0064	0.0083 ± 0.0088	0.0003 – 0.045
C5-alkene triol2	85	0.61	1.88 ± 4.13	0.015 – 27.7	59	0.062	0.13 ± 0.21	0.0051 – 1.07	37	0.0031	0.0065 ± 0.013	0.0003 – 0.077
C5-alkene triol3	96	0.57	10.4 ± 31.6	0.0025 – 221	59	0.12	0.28 ± 0.42	0.0039 – 1.99	67	0.017	0.033 ± 0.041	0.0021 – 0.18
∑C5-alkene triols	102	0.94	14.5 ± 43.9	0.016 – 318	77	0.093	0.41 ± 0.79	0.0042 – 4.92	73	0.017	0.037 ± 0.051	0.0003 – 0.24
2-methylthreitol	102	0.52	2.35 ± 3.60	0.042 – 21.8	95	0.047	0.41 ± 1.11	0.0009 – 7.12	61	0.026	0.19 ± 0.43	0.0016 – 2.44
2-methylerythritol	102	1.22	7.14 ± 13.4	0.10 – 87.2	80	0.15	0.89 ± 1.98	0.0008 – 11.6	65	0.047	0.55 ± 1.12	0.0064 – 6.25
∑2-methyltetrols	102	1.74	9.49 ± 16.9	0.16 – 109	96	0.15	1.15 ± 2.89	0.0009 – 18.7	66	0.061	0.72 ± 1.50	0.0016 – 8.01
Biomass burning tracer												
levoglucosan	102	45.3	65.9 ± 71.1	4.47 – 415	8	0.37	0.60 ± 0.74	0.018 – 2.28	63	0.015	0.023 ± 0.036	0.0025 – 0.25
Sugars and sugar alcohols												
meso-erythritol	102	0.93	1.15 ± 0.80	0.17 – 4.99	12	0.040	0.074 ± 0.085	0.0019 – 0.21	22	0.012	0.013 ± 0.012	0.0012 – 0.061
fructose	102	3.05	14.9 ± 62.9	1.12 – 473	60	0.055	0.11 ± 0.18	0.0008 – 1.21	64	0.054	0.12± 0.14	0.0003 – 0.59
mannose	102	0.33	0.41 ± 0.31	0.0021 – 1.62	37	0.0060	0.017 ± 0.026	0.00 – 0.13	62	0.0042	0.018 ± 0.063	0.00 – 0.38
glucose	102	7.46	13.8 ± 31.3	1.22 – 239	74	0.20	0.31 ± 0.35	0.0024 – 2.01	60	0.11	0.48 ± 0.87	0.0032 – 5.15
xylitol	92	0.81	0.89 ± 0.63	0.048 – 3.13	23	0.036	0.049 ± 0.048	0.0068 – 0.22	0	/	/	/
arabitol	102	5.13	7.35 ± 6.99	0.50 – 39.3	10	0.034	0.13 ± 0.22	0.0021 – 0.68	23	0.011	0.026 ± 0.034	0.0002 – 0.15
manitol	102	6.87	11.3 ± 11.6	0.65 – 74.2	18	0.072	0.091 ± 0.10	0.0040 – 0.43	56	0.060	0.10 ± 0.13	0.0058 – 0.63

Table S4. Predicted physicochemical properties of target polyol tracers.

Polyol species	**Molecular formula**	**MW**	$p^{o,*}_{L}$ [a] **(atm)**				$K^{*}_{H,w}$ [b] **(mol m^{-3} atm^{-1})**			ΔH^{*}_{sol} [c]	**Log** K_{OW}[d]
			EPI[e]	Evaporation[f]	SPARC[g]	SIMPOL[h]	EPI	SPARC	Literature values	(kJ mol^{-1})	
Isoprene SOA tracers											
cis-2-methyl-1,3,4-trihydroxy-1-butene[i]	$C_5H_{10}O_3$	118	1.89×10^{-7}	1.07×10^{-7}	2.40×10^{-9}	1.17×10^{-7}	1.28×10^{7}	3.76×10^{11}	1.9×10^{10}[j], 3.0×10^{10}[k]	-92.6	-0.90
3-methyl-2,3,4-trihydroxy-1-butene[i]	$C_5H_{10}O_3$	118	6.96×10^{-7}	7.76×10^{-7}	2.29×10^{-6}	1.17×10^{-7}	1.51×10^{7}	3.18×10^{7}		-92.6	-0.86
trans-2-methyl-1,3,4-trihydroxy-1-butene[i]	$C_5H_{10}O_3$	118	1.89×10^{-7}	1.07×10^{-7}	2.40×10^{-9}	1.17×10^{-7}	1.28×10^{7}	3.76×10^{11}		-92.6	-0.90
2-methylthreitol	$C_5H_{12}O_4$	136	2.28×10^{-8}	6.17×10^{-9}	4.68×10^{-9}	8.89×10^{-10}	2.44×10^{9}	3.36×10^{13}		-133	-1.65
2-methylerythritol	$C_5H_{12}O_4$	136	2.28×10^{-8}	6.17×10^{-9}	4.68×10^{-9}	8.89×10^{-10}	2.44×10^{9}	3.36×10^{13}		-133	-1.65
Biomass burning tracer											
levoglucosan	$C_6H_{10}O_5$	162	4.56×10^{-10}	2.69×10^{-9}	3.80×10^{-11}	2.42×10^{-9}	7.04×10^{12}	4.35×10^{15}	1.20×10^{11}[l]	-92.6	-1.25
Sugars and sugar alcohols											
meso-erythritol	$C_4H_{10}O_4$	122	6.91×10^{-10}	2.51×10^{-9}	4.37×10^{-10}		3.25×10^{9}	4.12×10^{13}	3.24×10^{9}[m], 1.10×10^{15}[n]	-133	-2.11
fructose	$C_6H_{12}O_6$	180	2.52×10^{-11}	6.46×10^{-13}	4.27×10^{-17}		1.03×10^{14}	1.62×10^{19}		-144	-1.55
mannose	$C_6H_{12}O_6$	180	2.13×10^{-11}	3.02×10^{-12}	6.92×10^{-15}		1.70×10^{10}	1.37×10^{18}		-144	-2.43
glucose	$C_6H_{12}O_6$	180	1.76×10^{-10}	6.92×10^{-14}	1.86×10^{-17}		1.03×10^{14}	1.81×10^{20}		-144	-2.89
xylitol	$C_5H_{12}O_5$	152	7.40×10^{-13}[o]	7.94×10^{-12}	4.68×10^{-13}		6.67×10^{10}	7.35×10^{16}	6.69×10^{10}[m], 4.00×10^{16}[n]	-140	-2.56
arabitol	$C_5H_{12}O_5$	152	2.07×10^{-13}[o]	7.94×10^{-12}	4.68×10^{-13}		6.67×10^{10}	7.35×10^{16}	6.80×10^{16}[n]	-147	-2.56
manitol	$C_6H_{14}O_6$	182	1.73×10^{-12}	2.51×10^{-14}	7.59×10^{-17}		1.38×10^{12}	1.04×10^{20}	1.42×10^{12}[m], 1.80×10^{20}[n]	-184	-3.01

[a] Liquid-state vapor pressure at 298.15 K; [b] Henry's law constant in pure water at 298.15 K; [c] enthalpy of dissolution, obtained from Compernolle and Müller (2014); [d] logarithm of *n*-octanol/water partition coefficient; [e] EPI: Estimation Programs Interface (EPI) Suite; [f] EVAPORATION: Compernolle et al. (2011). Values were obtained using the UManSysProp online tool (http://umansysprop.seaes.manchester.ac.uk/); [g] SPARC: Hilal et al. (1995, 2003, 2008). Values were obtained using the sparc online tool (http://archemcalc.com/sparc-web/calc); [h] SIMPOL: Pankow and Asher (2008); Values were obtained from Pye et al. (2018); [i] abbreviated as C5-alkene triol1, 2, and 3, respectively; [j] value of isoprene SOA from Vasilakos et al. (2021); [k] value of isoprene-derived epoxydiols (IEPOX) from Woo and Mcneill (2015) and Nguyen et al. (2014); [l] Gong (2018); [m] Sander (2015); [n] Compernolle and Müller (2014); [o] estimated as their solid-state vapor pressures from Compernolle and Müller (2014).

Table S5. Average relative uncertainties of measurements and calculated parameters.

Species	**$\Delta F/F$**[a]	**$\Delta A/A$**[b]	**$\Delta S/S$**[c]	**$\Delta F\%/F\%$**[d]	**$\Delta K/K$**[e]
Isoprene SOA tracers					
C5-alkene triol 1	0.028	0.032	0.027	0.037	0.043
C5-alkene triol 2	0.028	0.054	0.033	0.036	0.059
C5-alkene triol 3	0.028	0.077	0.034	0.038	0.084
2-Methylthreitol	0.028	0.051	0.028	0.033	0.059
2-Methylerythritol	0.028	0.066	0.030	0.035	0.072
Biomass burning tracer					
Levoglucosan	0.051	0.16	0.054	0.072	0.17
Sugars ang sugar alcohols					
Meso-erythritol	0.028	0.11	0.028	0.040	0.12
Fructose	0.23	0.27	0.26	0.31	0.36
Mannose	0.045	0.27	0.049	0.062	0.28
Glucose	0.094	0.28	0.10	0.18	0.31
Xylitol	0.10	0.12	0.10	0.14	0.16
Arabitol	0.097	0.26	0.099	0.14	0.28
Mannitol	0.21	0.42	0.21	0.29	0.47

[a] Particle-phase concentration; [b] gas-phase concentration; [c] total concentration; [d] particle-phase fraction; [e] partitioning coefficients of gas vs. organic and aqueous phases.

Figure S1

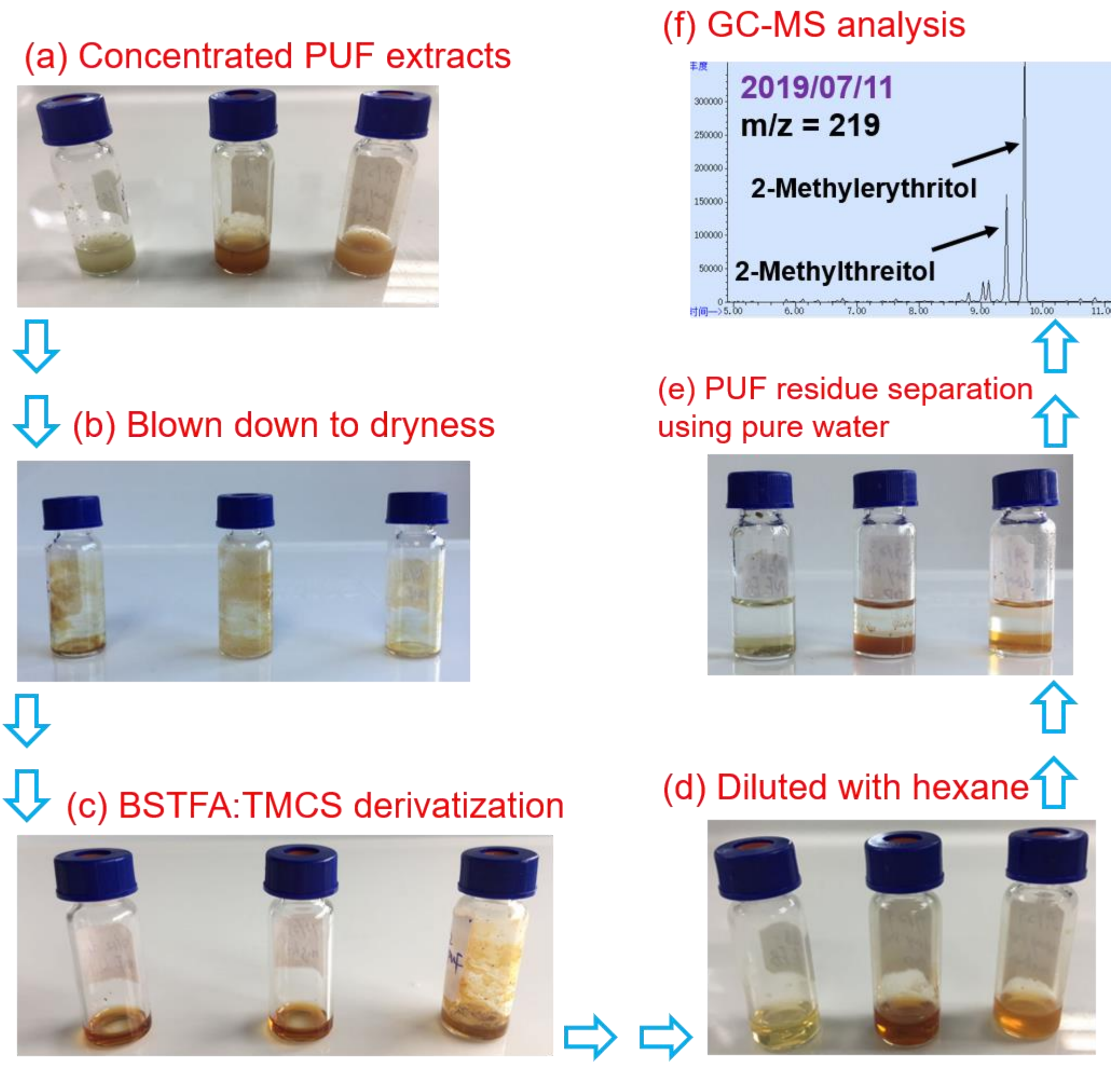

Figure S1. Revised procedures for analysis of gaseous polyols in PUF extracts.

Figure S2

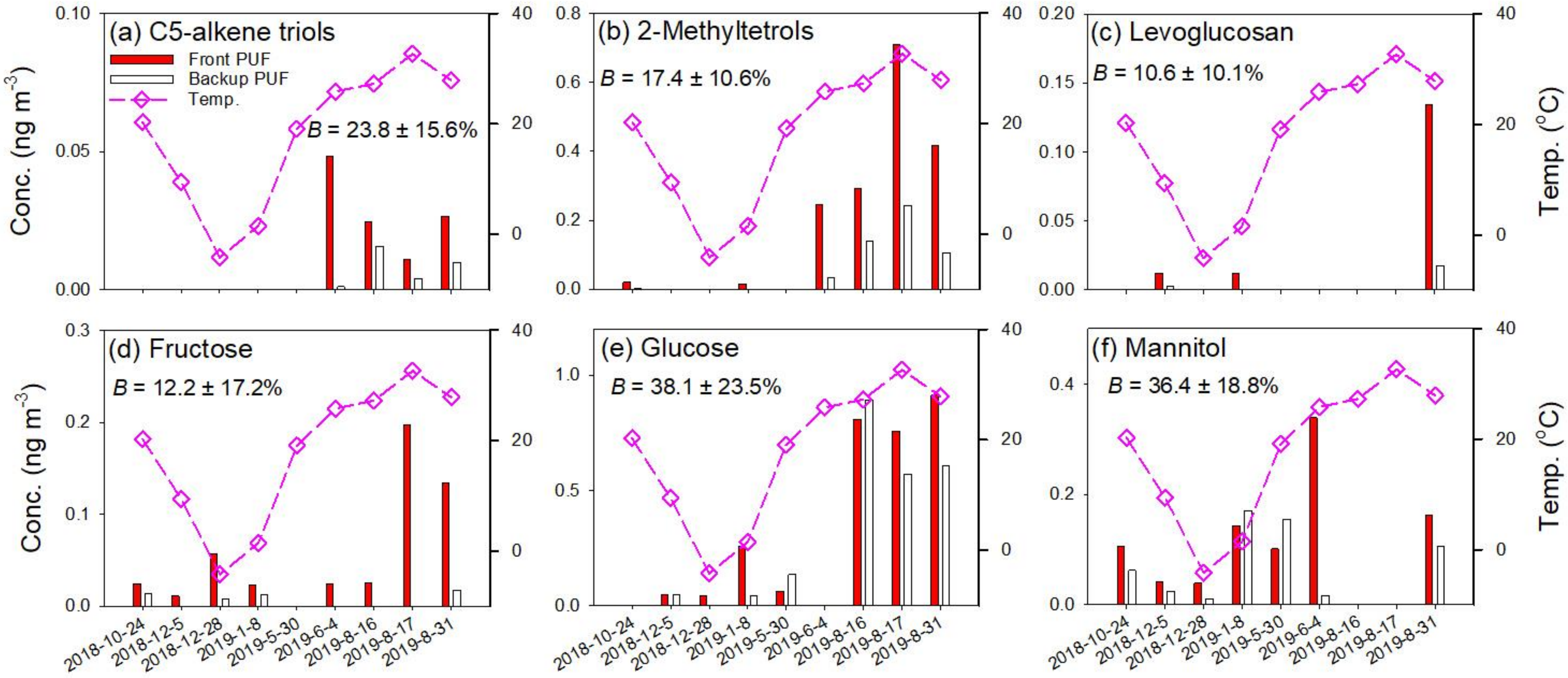

Figure S2. Concentrations of (a) C5-alkene triols, (b) 2-methylterols, (c) levoglucosan, (d) fructose, (e) glucose, and (f) mannitol in 9 pairs of front and backup PUF samples for breakthrough analysis.

Figure S3

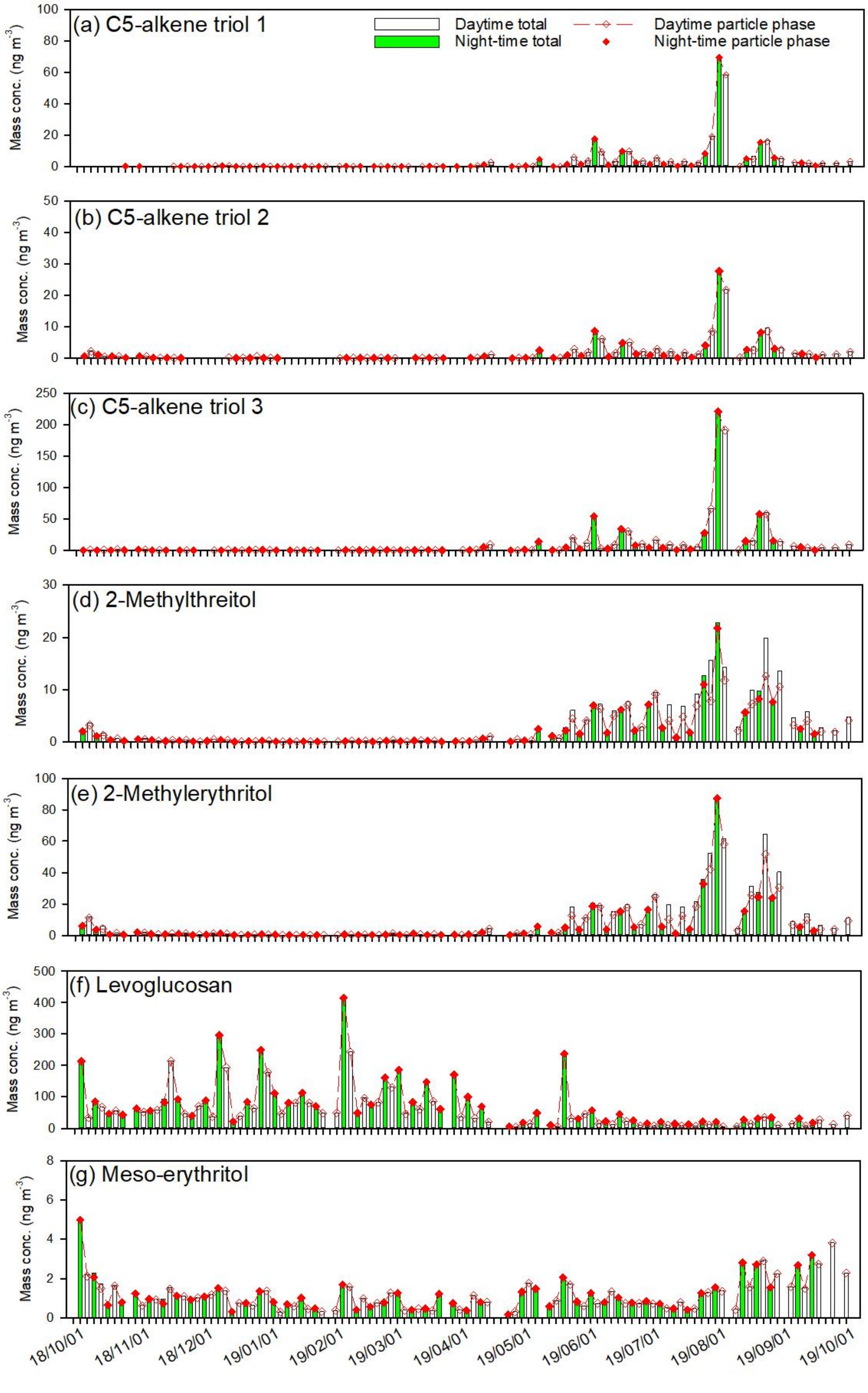

Figure S3. Temporal variations of total and Q_f concentrations of individual polyol tracers.

Figure S3 Continue

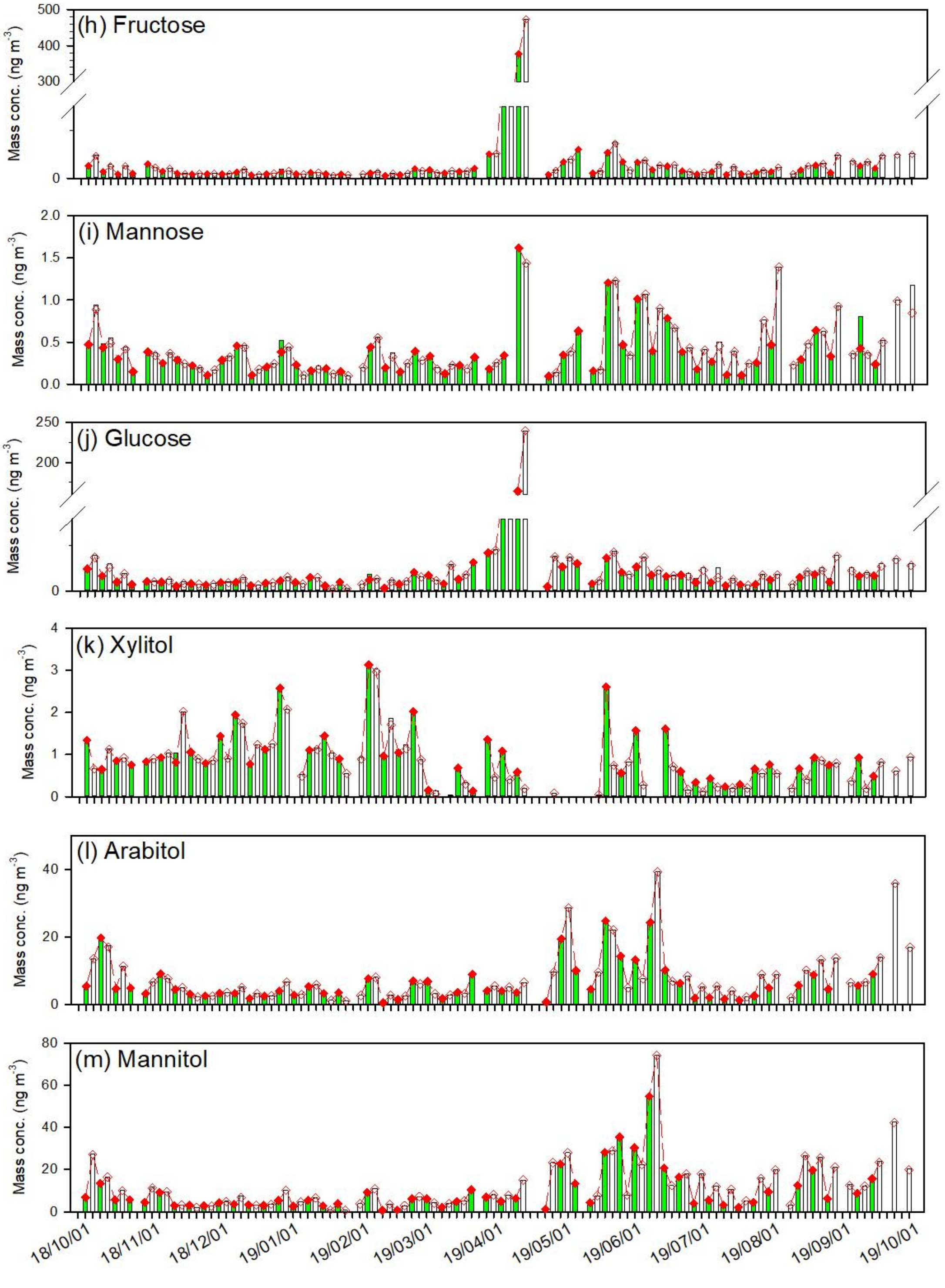

Figure S4

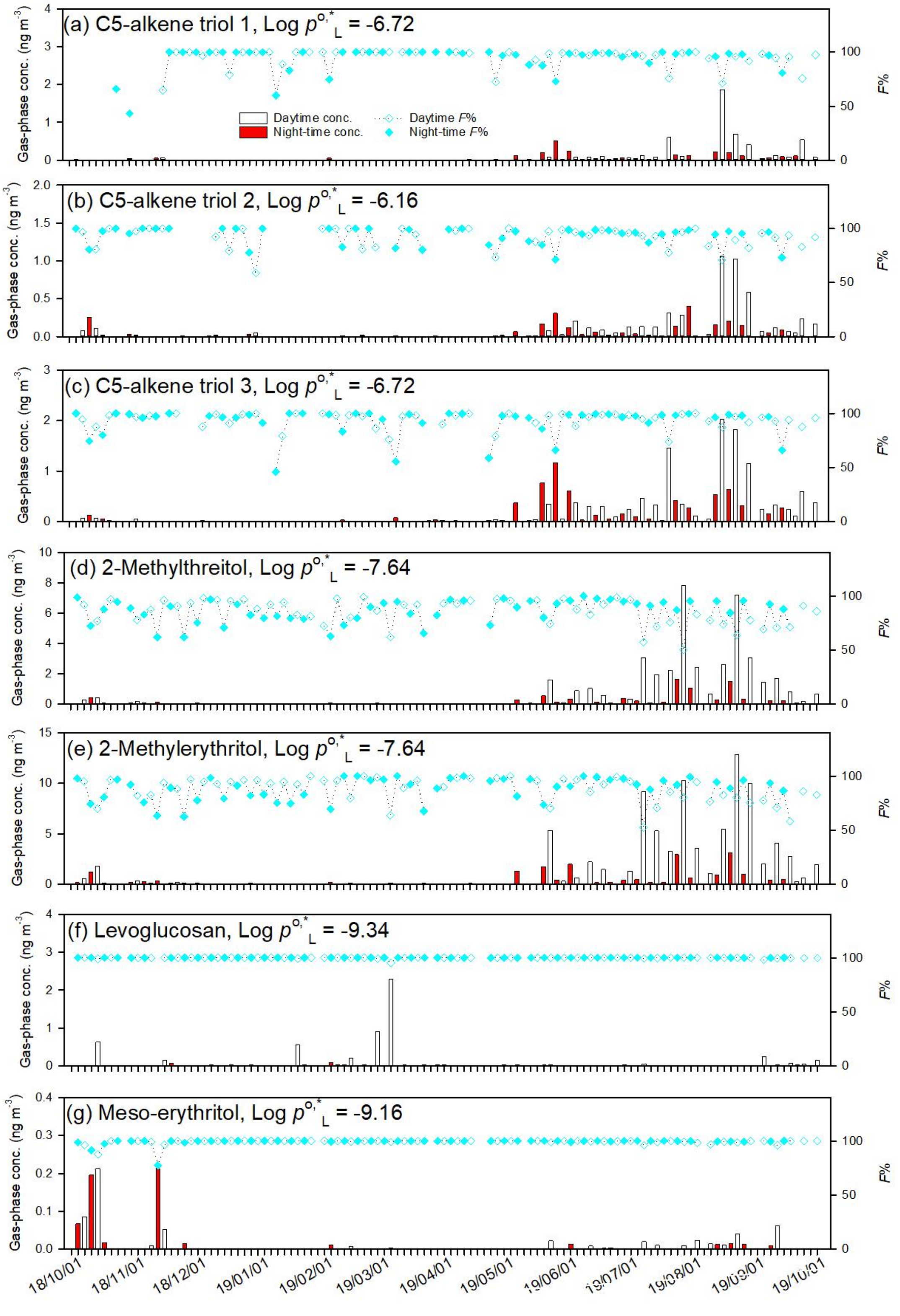

Figure S4. Temporal variations of gas-phase concentrations and particle-phase fractions (*F*%) of polyol tracers. $p^{o,*}_L$: Liquid-state vapor pressure (atm, EPI estimates) at 25 °C.

Figure S4 continue

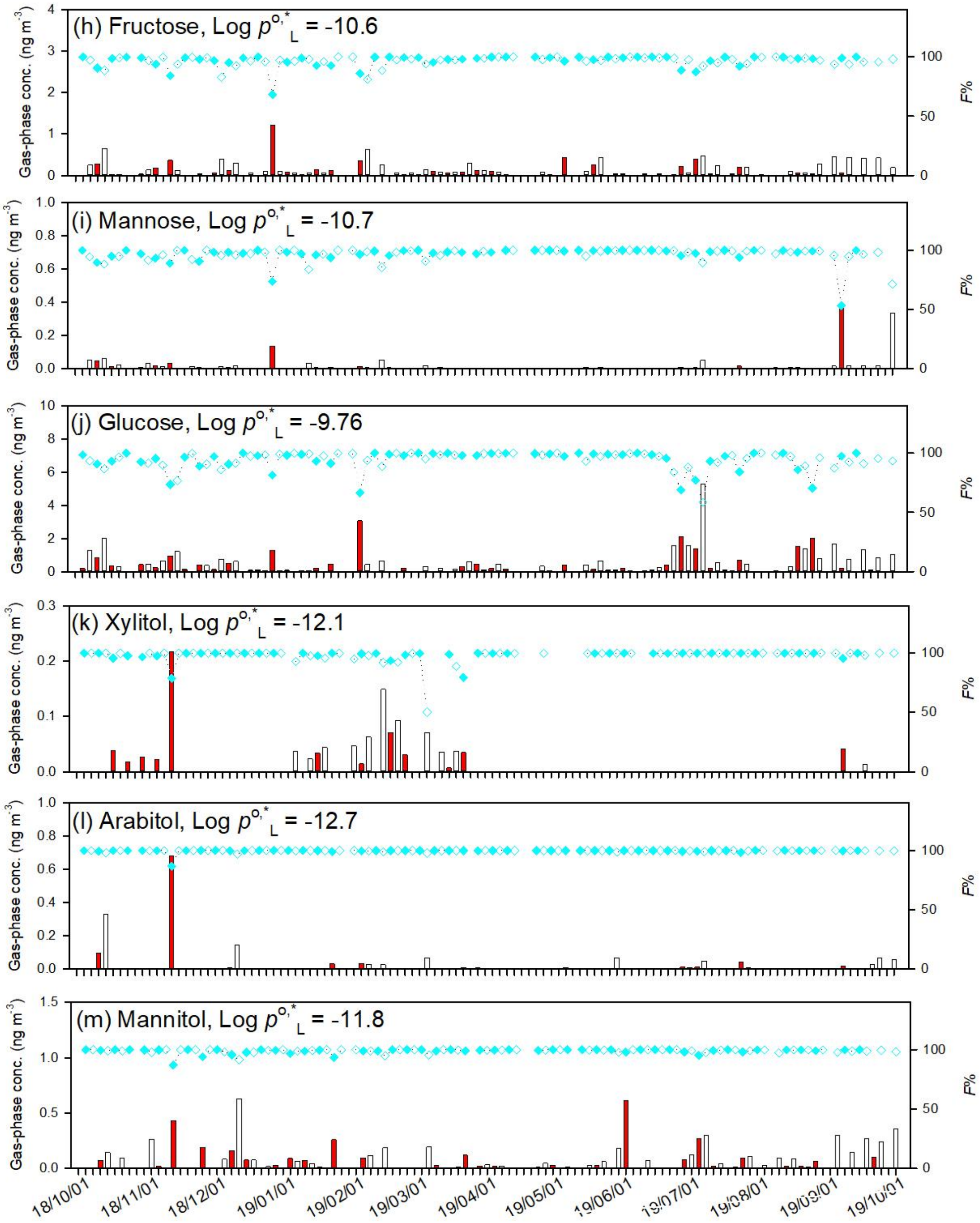

Figure S5

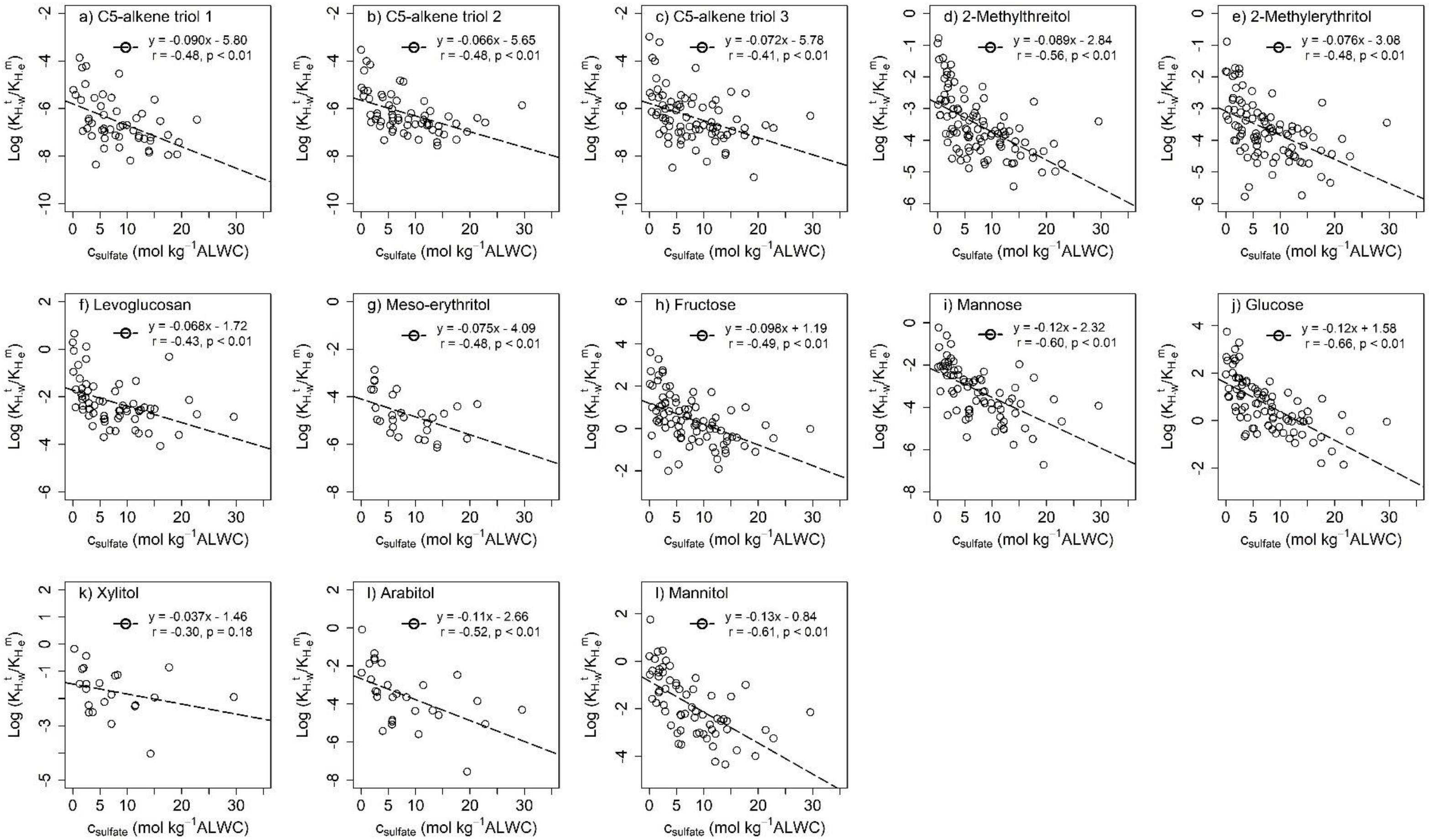

Figure S5. Modified Setschenow plots of log ($K^{t}_{H,w}/K^{m}_{H,e}$) vs. $c_{sulfate}$ for individual polyol tracers.

Figure S6

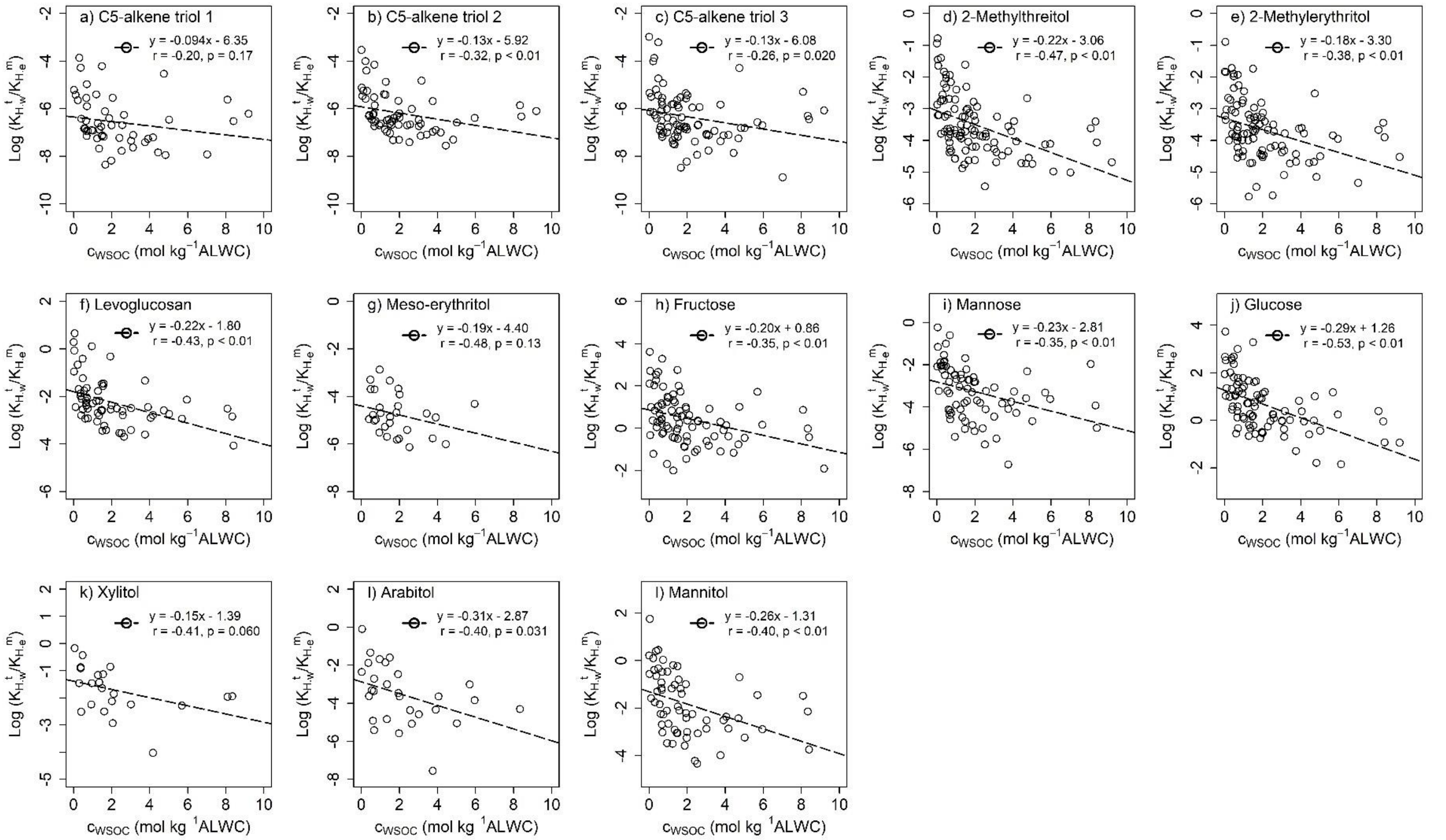

Figure S6. Linear regressions of log ($K^{t}_{H,w}/K^{m}_{H,e}$) vs. c_{WSOC} for individual polyol tracers (MW of WSOC was assumed as 200 g mol^{-1}).

References

Chang, R. Y. W., Slowik, J. G., Shantz, N. C., Vlasenko, A., Liggio, J., Sjostedt, S. J., Leaitch, W. R., and Abbatt, J. P. D.: The hygroscopicity parameter (κ) of ambient organic aerosol at a field site subject to biogenic and anthropogenic influences: relationship to degree of aerosol oxidation, Atmos. Chem. Phys., 10, 5047-5064, 10.5194/acp-10-5047-2010, 2010.

Claeys, M., Graham, B., Vas, G., Wang, W., Vermeylen, R., Pashynska, V., Cafmeyer, J., Guyon, P., Andreae, M. O., Artaxo, P., and Maenhaut, W.: Formation of secondary organic aerosols through photooxidation of isoprene, Science, 303, 1173-1176, 10.1126/science.1092805, 2004.

Compernolle, S., Ceulemans, K., and Müller, J. F.: EVAPORATION: a new vapour pressure estimation methodfor organic molecules including non-additivity and intramolecular interactions, Atmos. Chem. Phys., 11, 9431-9450, 10.5194/acp-11-9431-2011, 2011.

Compernolle, S., and Müller, J. F.: Henry's law constants of polyols, Atmos. Chem. Phys., 14, 12815-12837, 10.5194/acp-14-12815-2014, 2014.

Ding, X., Zheng, M., Yu, L., Zhang, X., Weber, R. J., Yan, B., Russell, A. G., Edgerton, E. S., and Wang, X.: Spatial and seasonal trends in biogenic secondary organic aerosol tracers and water-soluble organic carbon in the Southeastern United States, Environ. Sci. Technol., 42, 5171-5176, 10.1021/es7032636, 2008.

Ding, X., Wang, X.-M., Gao, B., Fu, X.-X., He, Q.-F., Zhao, X.-Y., Yu, J.-Z., and Zheng, M.: Tracer-based estimation of secondary organic carbon in the Pearl River Delta, south China, J. Geophys. Res. Atmos., 117, D05313, 10.1029/2011jd016596, 2012.

Dutton, S. J., Schauer, J. J., Vedal, S., and Hannigan, M. P.: PM2.5 characterization for time series studies: Pointwise uncertainty estimation and bulk speciation methods applied in Denver, Atmos. Environ., 43, 1136-1146, 10.1016/j.atmosenv.2008.10.003, 2009.

Gong, Z.: Gong, Z.: Uptake of organic molecules by atmospheric particles, Doctoral dissertation., https://dash.harvard.edu/handle/1/40050097, 2018.

Goss, K.-U., and Schwarzenbach, R. P.: Empirical prediction of heats of vaporization and heats of adsorption of organic compounds, Environ. Sci. Technol., 33, 3390-3393, 10.1021/es980812j, 1999.

Hilal, S. H., Karickhoff, S. W., and Carreira, L. A.: A rigorous test for SPARC's chemical reactivity models: Estimation of more than 4300 ionization pKas, Quant. Struct.-Act. Relat., 14, 348-355, 10.1002/qsar.19950140405, 1995.

Hilal, S. H., Karickhoff, S. W., and Carreira, L. A.: Prediction of the vapor pressure boiling point, heat of vaporization and diffusion coefficient of organic compounds, QSAR Comb. Sci., 22, 565-574, https://doi.org/10.1002/qsar.200330812, 2003.

Hilal, S. H., Ayyampalayam, S. N., and Carreira, L. A.: Air−liquid partition coefficient for a diverse set of organic compounds: Henry’s law constant in water and hexadecane, Environ. Sci. Technol., 42, 9231-9236, 10.1021/es8005783, 2008.

Hu, D., Bian, Q., Li, T. W. Y., Lau, A. K. H., and Yu, J. Z.: Contributions of isoprene, monoterpenes, β-caryophyllene, and toluene to secondary organic aerosols in Hong Kong during the summer of 2006, J. Geophys. Res. Atmos., 113, D22206, 10.1029/2008jd010437, 2008.

Isaacman-VanWertz, G., Yee, L. D., Kreisberg, N. M., Wernis, R., Moss, J. A., Hering, S. V., de Sá, S. S., Martin, S. T., Alexander, M. L., Palm, B. B., Hu, W., Campuzano-Jost, P., Day, D. A., Jimenez, J. L., Riva, M., Surratt, J. D., Viegas, J., Manzi, A., Edgerton, E., Baumann, K., Souza, R., Artaxo, P., and Goldstein, A. H.: Ambient gas-particle partitioning of tracers for biogenic oxidation, Environ. Sci. Technol., 50, 9952-9962, 10.1021/acs.est.6b01674, 2016.

Kleindienst, T. E., Jaoui, M., Lewandowski, M., Offenberg, J. H., Lewis, C. W., Bhave, P. V., and Edney, E. O.: Estimates of the contributions of biogenic and anthropogenic hydrocarbons to secondary organic aerosol at a southeastern US location, Atmos. Environ., 41, 8288-8300, 10.1016/j.atmosenv.2007.06.045, 2007.

Lin, Y. H., Knipping, E. M., Edgerton, E. S., Shaw, S. L., and Surratt, J. D.: Investigating the influences of SO2 and NH3 levels on isoprene-derived secondary organic aerosol formation using conditional sampling approaches, Atmos. Chem. Phys., 13, 8457-8470, 10.5194/acp-13-8457-2013, 2013.

Massoli, P., Lambe, A. T., Ahern, A. T., Williams, L. R., Ehn, M., Mikkilä, J., Canagaratna, M. R., Brune, W. H., Onasch, T. B., Jayne, J. T., Petäjä, T., Kulmala, M., Laaksonen, A., Kolb, C. E., Davidovits, P., and Worsnop, D. R.: Relationship between aerosol oxidation level and hygroscopic properties of laboratory generated secondary organic aerosol (SOA) particles, Geophys. Res. Lett., 37, https://doi.org/10.1029/2010GL045258, 2010.

Nguyen, T. B., Coggon, M. M., Bates, K. H., Zhang, X., Schwantes, R. H., Schilling, K. A., Loza, C. L., Flagan, R. C., Wennberg, P. O., and Seinfeld, J. H.: Organic aerosol formation from the reactive uptake of isoprene epoxydiols (IEPOX) onto non-acidified inorganic seeds, Atmos. Chem. Phys., 14, 3497-3510, 10.5194/acp-14-3497-2014, 2014.

Pankow, J. F., and Asher, W. E.: SIMPOL.1: a simple group contribution method for predicting vapor pressures and enthalpies of vaporization of multifunctional organic compounds, Atmos. Chem. Phys., 8, 2773-2796, 2008.

Pye, H. O. T., Zuend, A., Fry, J. L., Isaacman-VanWertz, G., Capps, S. L., Appel, K. W., Foroutan, H., Xu, L., Ng, N. L., and Goldstein, A. H.: Coupling of organic and inorganic aerosol systems and the effect on gas–particle partitioning in the southeastern US, Atmos. Chem. Phys., 18, 357-370, 10.5194/acp-18-357-2018, 2018.

Sander, R.: Compilation of Henry's law constants (version 4.0) for water as solvent, Atmos. Chem. Phys., 15, 4399-4981, 10.5194/acp-15-4399-2015, 2015.

Taylor, N. F., Collins, D. R., Lowenthal, D. H., McCubbin, I. B., Hallar, A. G., Samburova, V., Zielinska, B., Kumar, N., and Mazzoleni, L. R.: Hygroscopic growth of water soluble organic carbon isolated from atmospheric aerosol collected at US national parks and Storm Peak Laboratory, Atmos. Chem. Phys., 17, 2555-2571, 10.5194/acp-17-2555-2017, 2017.

US EPA: Estimation Program Interface (EPI) Suite. Version v4.11, 2012. United States Environmental Protection Agency, Washington, DC, USA. https://www.epa.gov/tsca-screening-tools/download-epi-suitetm-estimation-program-interface-v411

Vasilakos, P., Hu, Y., Russell, A., and Nenes, A. J. A.: Determining the role of acidity, fate and formation of IEPOX-derived SOA in CMAQ, Atmosphere, 12, 707, https://doi.org/10.3390/atmos12060707, 2021.

Woo, J. L., and McNeill, V. F.: simpleGAMMA v1.0 – a reduced model of secondary organic aerosol formation in the aqueous aerosol phase (aaSOA), Geosci. Model Dev., 8, 1821-1829, 10.5194/gmd-8-1821-2015, 2015.

Xie, M., Barsanti, K. C., Hannigan, M. P., Dutton, S. J., and Vedal, S.: Positive matrix factorization of PM2.5 - eliminating the effects of gas/particle partitioning of semivolatile organic compounds, Atmospheric Chemistry and Physics, 13, 7381-7393, 10.5194/acp-13-7381-2013, 2013.

Xie, M., Hannigan, M. P., and Barsanti, K. C.: Impact of Gas/Particle Partitioning of Semivolatile Organic Compounds on Source Apportionment with Positive Matrix Factorization, Environmental Science & Technology, 48, 9053-9060, 10.1021/es5022262, 2014a.

Xie, M., Hannigan, M. P., and Barsanti, K. C.: Gas/particle partitioning of 2-methyltetrols and levoglucosan at an urban site in Denver, Environ. Sci. Technol., 48, 2835-2842, 10.1021/es405356n, 2014b.

Yang, L., Shang, Y., Hannigan, M. P., Zhu, R., Wang, Q. g., Qin, C., and Xie, M.: Collocated speciation of PM2.5 using tandem quartz filters in northern nanjing, China: Sampling artifacts and measurement uncertainty, Atmos. Environ., 246, 118066, https://doi.org/10.1016/j.atmosenv.2020.118066, 2021.